COMMUNICATIONS IN SCIENCE AND TECHNOLOGY
Homepage: cst.kipmi.or.id

Efficient lead removal from industrial wastewater using activated carbon synthesized from wood sawdust

Firdos M. Abdulla[a], Qusay Al-Obaidi[a,*], Maryam Al-Ameri[a], Mohd Shukor Salleh[b], M. N. Mohammed[c], Oday I. Abdullah[d,e,f], Faris H. Al-Ani[g]

[a]College of Chemical Engineering, University of Technology, Baghdad 10066, Iraq
[b]Fakulti Teknologi Dan Kejuruteraan Industri Dan Pembuatan, Universiti Teknikal Malaysia Melaka, Hang Tuah Jaya, Melaka 76100, Malaysia
[c]Mechanical Engineering Department, College of Engineering, Gulf University, Sanad 26489, Bahrain
[d]College of Engineering, Al-Naji University, Baghdad 10015, Iraq
[e]Department of Energy Engineering, College of Engineering, University of Baghdad, Baghdad 10071, Iraq
[f]Department of Mechanics, Al-Farabi Kazakh National University, Almaty 050040, Kazakhstan
[g]College of Civil Engineering, University of Technology, Baghdad 10066, Iraq

Article history:
Received: 13 February 2026 / Received in revised form: 18 June 2026 / Accepted: 19 June 2026

Abstract

The social economy's rapid expansion and unprecedented population growth are significantly contributing to environmental issues. Contamination of soil and water by heavy metals is a major environmental problem. Activated carbon synthesized from biomass possesses several qualities, including a large specific surface area, a hierarchically porous structure, robust adsorption capability, and high economic value. Wood sawdust, a plentiful agricultural by-product, was used to chemically produce activated carbon (AC). Lead removal from industrial wastewater was examined using this AC. The Langmuir and Freundlich models, along with first- and second-order kinetics, were applied for kinetic analysis. The novelty of this work lies in the combination of moderate-temperature chemical activation (600 °C) with Iraqi wood sawdust, achieving a remarkably high surface area (1477.54 m^2/g) compared to most previously reported biomass-derived adsorbents. Results showed an impressive maximum adsorption capacity of 177.54 mg/g. This value compares favorably with many recently reported biomass-derived adsorbents. The boundary layer effect occurs, and the adsorption of Pb follows pseudo-second-order kinetics.

Keywords: Lead; activated carbon; wood sawdust; adsorption isotherm; kinetics

1. Introduction

The metal plating, mining, pigment, and fertilizer sectors have expanded rapidly in recent years. As a result, heavy metal-contaminated water is now considered one of the most severe environmental issues, involving zinc (Zn), mercury (Hg), copper (Cu), chromium (Cr), lead (Pb) [1], cadmium (Cd), nickel (Ni), and manganese (Mn) [2,3]. These heavy metals cannot biodegrade and accumulate in living beings, posing a significant threat to both humans and the biota [4,5]. Lead (Pb (II)) is frequently found in alloys (0.07–1.0%) [6], batteries (70%), and numerous ores (4%) [7]. Lead pollution is also caused by mining, ore manufacturing, hazardous disposal of industrial effluents [8], use of lead compounds as paint pigments, and anti-knock agents in gasoline.

* Corresponding author.
Email: qusay.j.alobaidi@uotechnology.edu.iq
https://doi.org/10.21924/cst.11.1.2026.1914

Lead affects the gastrointestinal tract, liver, kidneys, and central nervous system [4,9-10]. The US Environmental Protection Agency's (EPA) guidelines highlight that lead levels in drinking water should stay below 0.05 mg/L [11-13]. Adsorption is a highly economical and efficient method for removing heavy metals [14]. Recent adsorption investigations have focused on optimizing adsorbent synthesis and enhancing their selectivity [15-18].

Despite numerous studies on biomass-derived activated carbon for Pb(II) removal, the specific combination of Iraqi wood sawdust as a precursor with chemical activation at 600 °C under controlled N_2 flow (130 mL/min) has not been systematically investigated. In addition, the values reported for both surface area and maximum adsorption capacity, 1470 m2/g and 177.54 mg/g, respectively, are notably higher than several previous studies (usually Qmax of 75-125 mg/g), proving the novelty of the synthesising method. This study aims to: 1- evaluate the lead adsorption capacity of activated carbon

This open access article is distributed under a Creative Commons Attribution (CC-BY) 4.0 license

synthesized from locally available wood sawdust, 2- determine the best-fitting kinetics and isotherm models, and 3- provide a mechanistic insight into the adsorption process using both model fitting and FTIR/XRD characterization.

The novelty is not the general use of biomass-derived activated carbon, but rather the specific use of locally available Iraqi wood sawdust under moderate activation conditions, with competitive Pb(II) capacity.

2. Materials and Methods

2.1. Lead solution preparation

1.5984 grams of $Pb(NO_3)_2$ were diluted in distilled water to generate a stock solution that contained 1 mg of lead per Cm^3, then filled to 1 L. Distilled water was used to dilute further to produce lower concentrations (500-200 mg dm^{-3}). All chemicals were of analytical grade. 5 mL of concentrated HNO_3 was added to prevent hydrolysis [19,20].

2.2. Batch adsorption experiments

For kinetic testing, 0.2 g of adsorbent was used in flasks containing 200 mL of solutions with 200 mg/L lead ion (Pb^{2+}). Pb^{2+} concentration was measured spectrophotometrically using 1 mL aliquots at appropriate time intervals [21,22]. A Varian AA250 Plus atomic absorption spectrophotometer with an air-acetylene flame was utilized for final Pb(II) measurements. Adsorption percentage was calculated as [23]:

$$\text{Adsorption (\%)} = \frac{(C_{int} - C_{fin})}{C_{int}} * 100 \quad (1)$$

where C_{int} and C_{fin} represent the initial and end lead concentrations [16].

The amount of adsorbed lead was computed using the following formula,

$$qe = \frac{V(C_0 - C_e)}{W} \quad (2)$$

where W is the adsorbent mass (g), V is the solution volume (L), and C_0 and C_e represent the concentrations at initial and equilibrium (mg L^{-1}).

2.3. Activated carbon preparation

Wood sawdust waste residue was acquired from a local furniture shop in Baghdad, Iraq. Samples were washed with deionized water, dried, mechanically ground, and sieved to 1-2 mm particles, then dried for 24 hr at 110 °C. A tubular horizontal furnace carbonized the sample for 1 hr at 600 °C under N_2 flow (130 mL/min).
Yield was calculated as [13]:

$$\text{Yield}(\%) = 100 * \left(\frac{Wc}{W0}\right) \quad (3)$$

where W_c is the final dry weight, and W_0 is the precursor dry weight.

3. Results And Discussions

3.1. Characterization of activated carbon

(FTIR) Fourier transform infrared spectroscopy (IRAffinity-1-SHMADZo) assessed the functional group loading within 4000-400 cm^{-1}, N_2 adsorption/desorption (Micromeritics Tristar II 3020 V1.03) was performed after outgassing at 300 °C for 1 hr. The Brunauer-Emmett-Teller (BET), surface area (SSA), and micropore volume are adequate for achieving maximum values of 1470 m^2/g and 0.562 cm^3/g, respectively, significantly higher than many previously reported biomass-derived activated carbons (typically 800-1200 m^2/g [24-26].

Furthermore, X-ray diffraction (Fig. 2) revealed two broad peaks corresponding to the (002) and (10) Bragg reflections at ~26° and ~44°, indicating the amorphous nature of activated carbons [26-29]. The broad (002) lines result from a few stacked layers, and asymmetric (10) lines from random turbostratic layer stacking. Some sharp peaks correspond to residual ash [30-32]. Direct evidence from FTIR (Fig. 1) shows characteristic peaks at ~300 and ~400 cm^{-1} (O-H) stretching of hydroxyl and carboxyl groups, ~1700 cm^{-1} (C=O stretching of carbonyl/carboxyl), confirming the presence of oxygen-containing functional groups that serve as active sites for Pb(II) coordination.

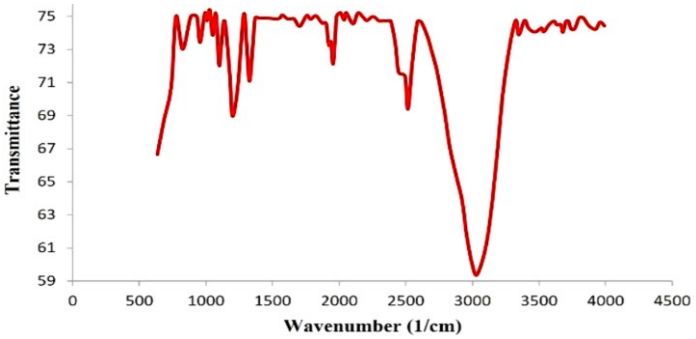

Fig. 1. FTIR diagrams for the prepared activated carbon (A.C)

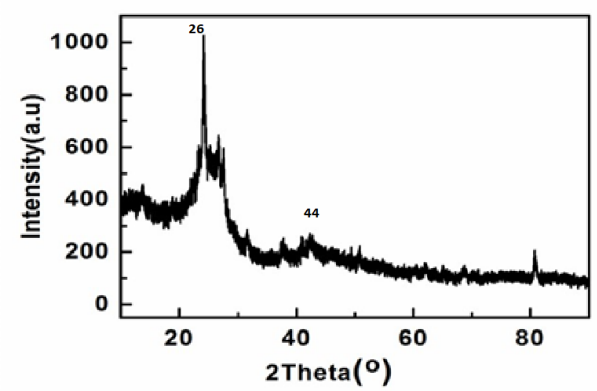

Fig. 2. X-ray diffraction profile of the prepared A.C

3.2. Batch equilibrium studies

Adsorption capacity was calculated using Eq. (4). Each experiment was repeated with a maximum variance of 5%.

$$q_e = \frac{(C_0 - C_e)V}{m} \quad (4)$$

Here, V represents the solution's volume, expressed in liters, whereas m is the amount of adsorbent, which is measured in g, and C_o and C_e represent the initial and final concentrations, respectively. Each adsorption experiment was repeated with a maximum variance of 5%.

3.3. Removal percentage of lead

Fig. 3 shows that with increasing $Pb(NO_3)_2$ concentration from 100 mg/L to 500 mg/L, the removal percentage increased to a peak of 83% at 300 mg/L, then decreased to ~77%. The primary rise in the removal percentage because the mass transfer force exceeds the film resistance force. Beyond 300 mg/L, active surface sites are filled with lead (II) ions, causing saturation and site limitation [33].

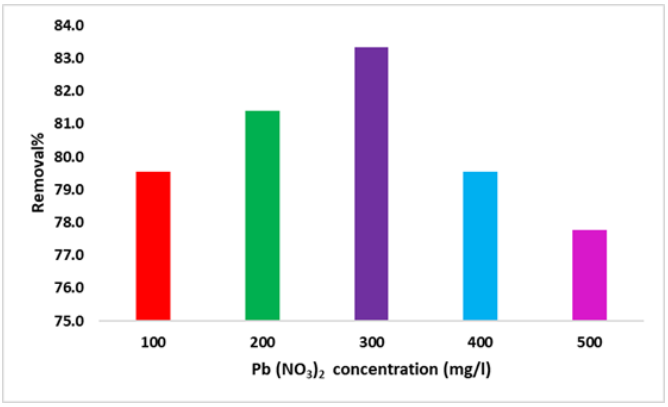

Fig. 3. Removal of lead (II) ion after the exhaustion of the adsorption process for 7 hours

3.4. Adsorption isotherm models

At a temperature that remains constant, the adsorption isotherm is a mathematical statement. The result can be used to calculate the equilibrium capacity for adsorption, which is also referred to as (qe). Additionally, it determines the concentration of adsorbate at equilibrium concentration, denoted by (Ce). This first one is a representation of the relationship that exists between the two quantities.

3.4.1. Langmuir isotherm

The Langmuir isotherm model can be expressed as follows in its linear form:

$$\frac{C_e}{q_e} = \frac{1}{Q_{max}\,K_l} + \left(\frac{1}{Q_{max}}\right) C_e \qquad (5)$$

The ratio of the amount of adsorbate that is adsorbed to the total mass of the adsorbent is given by the symbol Ce; q_e. The equilibrium concentration of the adsorbate is measured in mg/L. The Langmuir constants Q_{max} and K_l correspond to the adsorbent's affinity for the adsorbate and monolayer adsorption capacity, respectively.

3.4.2. Freundlich isotherm

The following is an expression of the logarithmic form of the Freundlich model:

$$log\, q_e = log\, K_F + \frac{1}{n} log\, C_e \qquad (6)$$

The equilibrium adsorption capacity (mg/g) is denoted by qe; Ce is the equilibrium concentration of the adsorbent, while KF and n are the Freundlich constants.

Monolayer adsorption of Pb^{2+} ions onto a homogeneous distribution of active sites on the activated carbon surface. The maximum monolayer adsorption capacity (Qmax) obtained from the linearized Langmuir plot was 177.54 mg/g, which reflects the highest theoretical amount of Pb^{2+} that can be adsorbed per unit mass of the prepared activated carbon under the studied conditions.

3.4.3. Langmuir maximum adsorption capacity (Qmax)

The Langmuir isotherm model provided the best fit for the equilibrium adsorption data, confirming monolayer adsorption of Pb^{2+} ions onto a homogeneous distribution of active sites on the activated carbon surface. According to the Langmuir model assumes that adsorption occurs uniformly on energetically identical binding sites, where no interaction occurs between adsorbed molecules.

This high Qmax value demonstrates the strong affinity between Pb^{2+} ions and the functional groups present on the activated carbon, particularly hydroxyl, carbonyl, and carboxylic groups introduced during chemical activation. Similar findings were reported by Wu, Tseng, and Juang [34], who highlighted the major role of oxygenated surface groups in enhancing heavy-metal chemisorption. The large BET surface area, well-developed microporous structure, and uniform pore distribution further contribute to the enhanced adsorption capacity by increasing the number of active sites and facilitating rapid ion diffusion within the pores, which is consistent with the observations of Saleh[35] regarding the relationship between pore structure and adsorption performance.

Table 1. Several studies of lead (II) ion adsorption using biomass-derived activated carbon as an adsorbent

Precursor Biomass of (AC)	Activation Method	Qmax (mg/g)	Reference
Coconut shell	H_3PO_4 activation	33.40–175.63	[38]
Rice husk	Thermal activation	75.5	[39]
Date pits	ZCPs activation	247.75	[40]
Pine sawdust	H_2SO_4 activation	26.50	[19]
Mixed agricultural AC	Chemical activation	97–140	[6]
Biomass-derived activated carbons	Various activation methods	Variable adsorption capacities reported for Pb(II) removal >99%	[41]
Clinoptilolite/Biochar/$Ca(OH)_2$ composite	Composite modification	Pb(II) removal efficiency	[33]
Commercial AC (coal-based)	Steam activation	80-100	Various sources
Wood sawdust (Iraq)	Chemical activation + 600°C	177.54	Present work

Compared with previously reported biomass-derived activated carbons, the Qmax value obtained in this study is significantly higher, where typical Qmax values range between 75 and 125 mg/g for adsorbents such as rice husk, coconut shell, and pine sawdust carbons [36,37]. The superior adsorption performance observed here highlights the effectiveness of the activation method and confirms the strong potential of wood-sawdust-derived activated carbon as a highly efficient and low-cost adsorbent for heavy-metal removal from aqueous environments, as shown in Table 1.

The Langmuir isotherm model described the adsorption process accurately (R^2=0.998, Table 2), demonstrating a monolayer of Pb^{2+} ions adheres onto a homogeneous distribution of active sites on the A.C. reaching (Qmax) of 177.54 mg/g.

As Table 1 shows, the current sawdust-derived activated carbon has a competitive capability to adsorb Pb(II) in contrast with other reported bio-based A.C and previously published adsorbents.

3.5. *Adsorption kinetic*

3.5.1. *Pseudo-first-order kinetic model*

$$log(q_e - q_t) = log\, q_e - \frac{K_1}{2.303}\, t \qquad (7)$$

In this equation, qe and q_t refer to the quantity of copper adsorbed (mg/g) at equilibrium and time t. Furthermore, the rate constant of the adsorption is denoted by k_1. The value of k_1 was determined by plotting log (qe - qt) and t for different concentrations of Pb.

3.5.2. *Pseudo-second-order kinetic model*

$$\frac{1}{q_t} = \frac{1}{k_2 q_e^2} + \frac{1}{q_2}\, t \qquad (8)$$

In this equation, qe and q_t refer to the quantity of copper adsorbed (mg/g) at equilibrium and time t. Furthermore, the rate constant of the adsorption is denoted by k_2.

3.6. *Adsorption isotherms*

Adsorption is an extensively used separation method because of its low cost and excellent effectiveness, particularly in environmental remediation. Adsorption isotherm models can provide mechanistic knowledge about the adsorption process, which is essential for developing adsorption systems. According to the Temkin isotherm model, adsorbate-adsorbate interactions cause the heat of adsorption of molecules in a layer to drop linearly with coverage. This model works well at modest coverage levels and considers the indirect interactions between adsorbed molecules. The Temkin isotherm (R^2=0.9872) and the Dubinin-Radushkevich isotherm (R^2=0.865) were also evaluated (Fig. 4, Table 2).

3.7. *Adsorption kinetics results*

The study of how fast an adsorbent takes up molecules of an adsorbate is known as adsorption kinetics. Knowledge of adsorption kinetics is essential when developing and refining adsorption procedures for uses such as water purification [42,43]. An important part of adsorption kinetics is the adsorption rate, or the rate at which adsorption occurs. Considerations such as adsorbate concentration, surface area, and temperature play a significant role. The adsorption kinetics are affected by several factors, such as the adsorbate's composition, the adsorbent's surface characteristics, temperature, pH, and competing ions or molecules. Kinetic parameters are summarized in Fig. 5 and Table 3. It shows that the pseudo-second-order model (R^2 >0.97) matches the reaction much better than the pseudo-first-order model (R^2 lower) consistently across all concentrations.

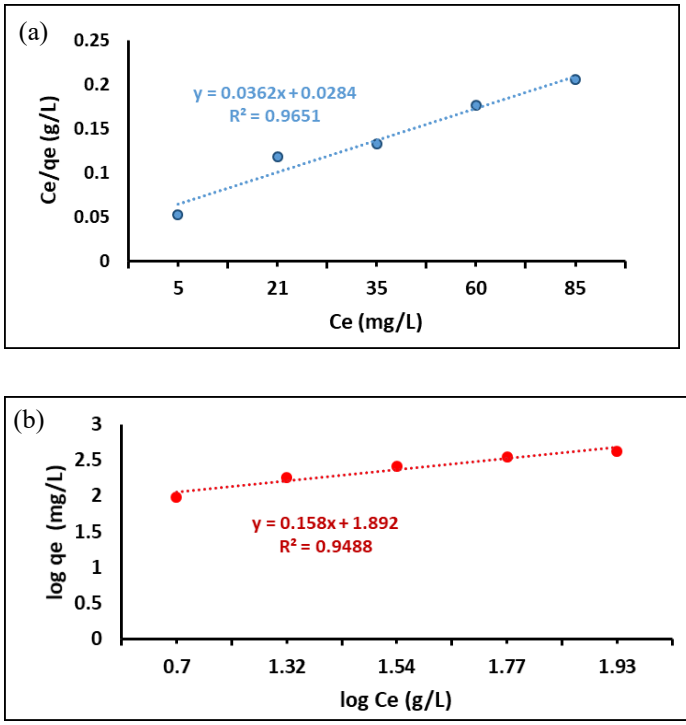

Fig. 4. Isotherms of Pb adsorption on AC at a temperature of 30 °C measured by Langmuir (a) and Freundlich (b)

Table 2. Isotherm model parameters for Pb adsorption on synthesized AC

Isotherm model	Parameter	Value	R^2
Langmuir	Qmax (mg/g)	177.54	0.998
	K_l (L/mg)	0.556	
Freundlich	K_F(mg/g(L/mg)$^{1/n}$	97.65	0.775
	n	0.122	
Temkin	K_T (L/g)	0.0776	0.9872
	B_T (J/mol)	78.213	
Dubinin–Radushkevich	qs (mg/g)	12.23	0.865
	−B	0.398	

3.8. *Adsorption mechanism*

While the pseudo-second-order kinetic model (R^2 > 0.99) is often associated with chemisorption, kinetic fitting alone is insufficient to definitively prove a specific adsorption mechanism. This study demonstrates that, in addition to the significant contribution of chemisorption to Pb(II) adsorption, the surface complexation, pore diffusion, and electrostatic interactions formed the overall removal mechanism, as proved by the results of both FTIR and isotherm analysis. The sequence

of mass-transfer and surface-interaction processes is responsible for Pb^{2+} adsorption:

-Film diffusion Pb^{2+} ions diffuse from the bulk solution toward the external surface.
-Intraparticle diffusion-Ions migrate into micro-and mesopores.
-Surface complexation-Ions interact with oxygen-containing functional groups.

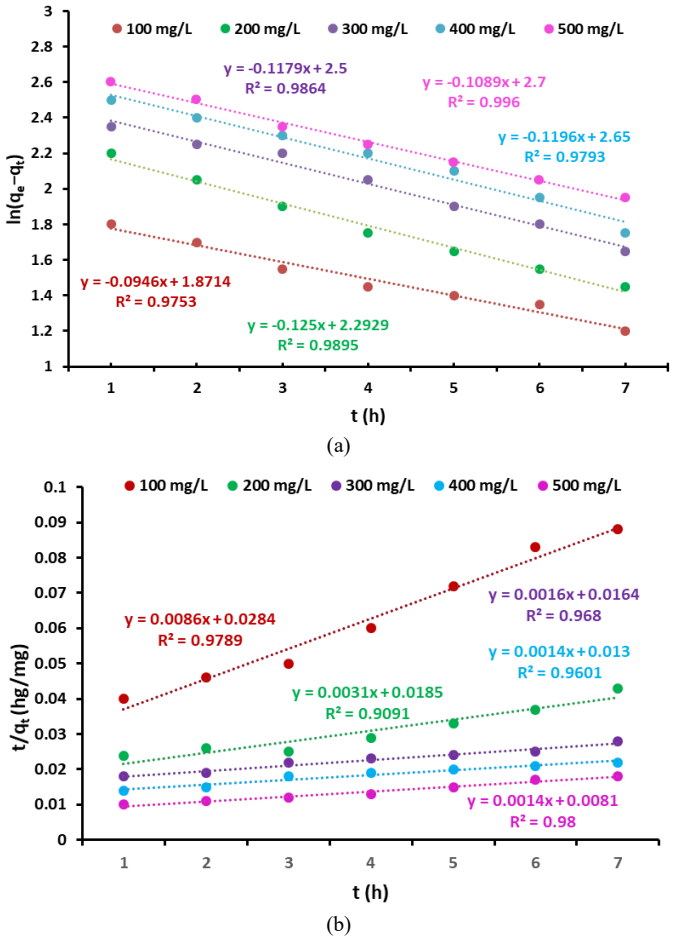

Fig. 5. The adsorption of Pb on AC at 30 °C is modelled using Pseudo-first-order (a), Pseudo-second-order, and kinetic techniques (b).

Table 3. Kinetic parameters for lead adsorption on A.C

Model	Parameter	Initial Concentration of Lead (mg/L)				
		100	200	300	400	500
Pseudo-first-order	qe, exp (mg/g)	32.54	50.75	43.98	32.67	45.84
	qe, cal (mg/g)	30.11	50	42.32	32.01	45.22
	K1 (1/h)	0.451	0.438	0.547	0.49	0.543
	R^2	0.978	0.909	0.968	0.96	0.98
	SSE (%)	42.98	45.18	47.67	48.23	50.78
Pseudo-second-order	qe, exp (mg/g)	22.532	25.344	22.391	24.768	25.331
	qe, cal (mg/g)	22.1	24.91	22.132	25.01	25.888
	K_2 (g/mg h)	0.046	0.047	0.06	0.058	0.048
	R^2	0.975	0.989	0.986	0.979	0.996
	SSE (%)	5.01	7.43	9.54	11.09	12.45

FTIR analysis (Fig. 1) demonstrates direct proof for the involvement of specific functional groups. The broadband at ~3400 cm^{-1} (O–H) stretching and peaks at ~1700 cm^{-1} (C=O), and ~1100 cm^{-1} (C–O) showed shifts after Pb^{2+} adsorption, indicating coordination band formation. FTIR analysis provides evidence that chemisorption may participate in the adsorption process, consistent with the pseudo-second-order kinetic fit. However, physical adsorption through electrostatic attraction and van der Waals interactions may also contribute, particularly at lower concentrations.

The high BET surface area (1470 m^2/g) and well-developed microporous volume (0.562 cm^3/g) increase available adsorption sites. The excellent agreement with the Langmuir isotherm (R^2=0.998) suggests a monolayer formation on energetically similar sites. The mean free energy (E) calculated from the D-R isotherm was approximately 8-16 kJ/mol (B=0.398, $E=1/\sqrt{(-2B)}$ ~11.2 KJ/mol), which falls within the range for ion-exchange and chemisorption processes (8-16 KJ/mol), further supporting the proposed mechanism. Fig. 6 representing of Pb^{+2} adsorption onto activated carbon [36]. The process includes film diffusion, intraparticle diffusion through micro-and mesopores, and surface complexation with functional groups.

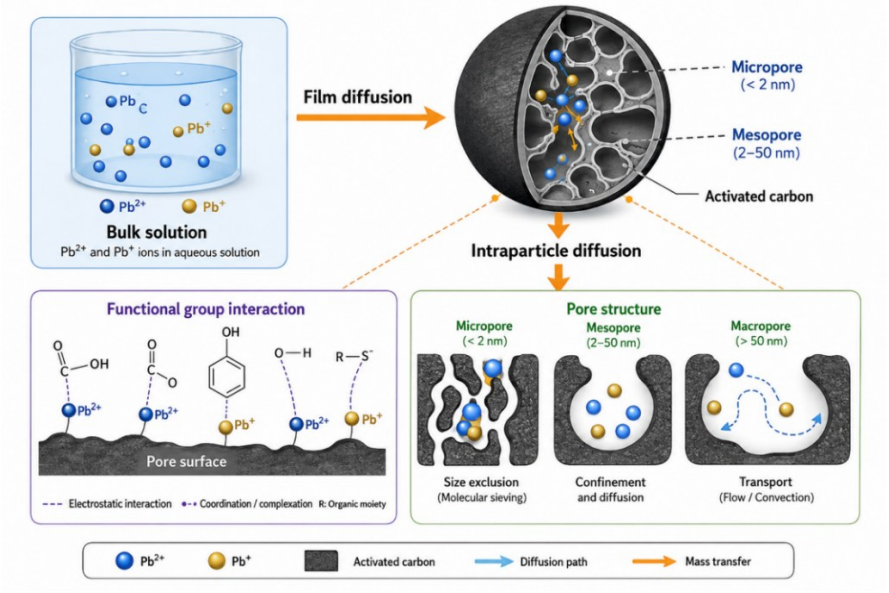

Fig. 6. The adsorption of Pb^{2+} ions onto activated wood sawdust

The study showed excellent Pb(II) adsorption performance; the mechanism was primarily determined using kinetic, isotherm, FTIR, and XRD investigations. Future research should incorporate post-adsorption FTIR, XPS, and regeneration investigations to further evaluate the adsorption process and long-term application of the adsorbent.

4. Conclusions

This study successfully demonstrated the efficient removal of Pb(II) from synthetic wastewater using activated carbon synthesized from Iraqi wood sawdust. The key findings are: The produced activated carbon exhibits a high surface area of 1470 m^2/g and a maximum adsorption capacity of 177.54 mg/g, which surpasses most previously reported biomass-derived adsorbents and several commercial activated carbons. The Langmuir isotherm model provided the best correlation (R^2 = 0.998), confirming a monolayer adsorption on homogeneous active sites. The pseudo-second-order kinetic model showed superior correlation ($R^2 > 0.98$) with significantly lower SSE values than the pseudo-first-order model, suggesting that surface interaction processes may play an important role. However, kinetic fitting alone cannot conclusively identify the adsorption mechanism. This interpretation is supported by FTIR evidence and D–R isotherm analysis ($E \approx 11.2$ kJ/mol). The combination of (i) high surface area, (ii) well-developed micro- and mesoporous network, and (iii) abundant oxygen-containing functional groups (hydroxyl, carbonyl, carboxylic) contributes to the superior adsorption performance. The novelty of this work lies in the specific activation conditions (600 °C, 130 mL/min N_2 flow) applied to locally available Iraqi wood sawdust, achieving performance metrics comparable to or better than more energy-intensive preparation methods.

Acknowledgments

The authors extend their appreciation to the University of Technology, Baghdad, Iraq.

Author Contributions

Firdos M. Abdulla: Conceptualization, Methodology, Investigation, Data Curation, Writing—Original Draft Preparation.; Qusay Al-Obaidi: Conceptualization, Validation, Writing—Review and Editing, Supervision.; Maryam Al-Ameri: Methodology, Investigation, Data Curation, Writing—Original Draft Preparation.; Mohd Shukor Salleh: Methodology, Resources, Writing—Review and Editing.; M. N. Mohammed: Validation, Formal Analysis, Writing—Review and Editing.; Oday I. Abdullah: Formal Analysis, Supervision, Data Curation, Visualization.; Faris H. Al-Ani: Resources, Supervision, Project Administration, Writing—Review and Editing.
All authors have read and agreed to the published version of the manuscript.

Conflicts of Interest

The authors declare no conflict of interest.

References

1. D.R. Wicakso, A. Mirwan, E. Agustin, N.F. Nopembriani, I. Firdaus, M. Fadillah, *Potential of silica from water treatment sludge modified with chitosan for Pb (II) and color adsorption in sasirangan waste solution*, Commun. Sci. Technol. 7 (2022) 188–193.
2. A.D. N'diaye, et al., *A review of biomaterial as an adsorbent: From the bibliometric literature review, the definition of dyes and adsorbent, the adsorption phenomena and isotherm models, factors affecting the adsorption process, to the use of typha species waste as adsorbent*, Commun. Sci. Technol. 7 (2022) 140–153.
3. M.N. Mohammed, O.I. Abdullah, M.J. Jweeg, H.S.S. Aljibori, T.A. Abdullah, N.M. Alawi, R.T. Rasheed, F. Meharban, H.T. Hamzah, Q. Al-Obaidi, *Comprehensive Review on Wastewater Treatment Using Nanoparticles: Synthesis of Iron Oxide Magnetic Nanoparticles, Publication Trends via Bibliometric Analysis, Applications, Enhanced Support Strategies, and Future Perspectives*, ASEAN J. Sci. Eng. 5 (2025) 1–30.
4. F. Fu, Q. Wang, *Removal of heavy metal ions from wastewaters: a review*, J. Environ. Manage. 92 (2011) 407–418.
5. Q. Al-Obaidi, N.Y. Selem, M.H. Al-Dahhan, *Emulsion liquid membrane (ELM) enhanced by nanoparticles and ionic liquid for extracting vanadium ions from wastewater,* Environ. Sci. Pollut. Res. 31 (2024) 48576–48589.
6. A. Shahat, H.M.A. Hassan, H.M.E. Azzazy, E.A. El-Sharkawy, H.M. Abdou, M.R. Awual, *Novel hierarchical composite adsorbent for selective lead (II) ions capturing from wastewater samples*, Chem. Eng. J. 332 (2018) 377–386.
7. M. Miler, Š. Bavec, M. Gosar, *The environmental impact of historical Pb-Zn mining waste deposits in Slovenia*, J. Environ. Manage. 308 (2022) 114580.
8. D.R. Wicakso, A. Mirwan, E. Agustin, N.F. Nopembriani, I. Firdaus, M. Fadillah, *Potential of silica from water treatment sludge modified with chitosan for Pb(II) and color adsorption in sasirangan waste solution*, Commun. Sci. Technol. 7 (2022) 188–193.
9. R.M. Iqbal, W. Supriadi, R.Y.P. Burhan, S.D. Nurherdiana, R.E. Hidayati, S. Subaer, R. Bayuaji, H. Fansuri, *Fabrication and characterization of fly ash-based geopolymer and its performance for immobilization of heavy metal cations*, Commun. Sci. Technol. 7 (2022) 112–118.
10. C.O. Anıagor, M.C. Menkıtı, *Relational description of an adsorption system based on isotherm, adsorption density, adsorption potential, hopping number and surface coverage*, Sigma J. Eng. Nat. Sci. 38 (2020) 1073–1098.
11. Q. Al-Obaidi, D.S. Ibrahim, M.N. Mohammed, A.J. Sultan, F.H. Al-Ani, T.A. Abdullah, O.I. Abdullah, N.Y. Selem, *A comprehensive analysis of the hydrogen generation technology through electrochemical water and industrial wastewater electrolysis,* Pol. J. Chem. Technol. 26 (2024)
12. Q. Al-Obaidi, N.Y. Selem, O. Karai, K. Benabderazak, M. Al-Dahhan, *Enhanced the simultaneous recovery/extraction of combined heavy metals of lead and vanadium from synthetic wastewater using an emulsion liquid membrane (ELM) with nanoparticles and ionic liquid*, Appl. Water Sci. 15 (2025) 283
13. G.M. Kadum, S.A. Mahdy, E.H. Ali, *Antimicrobial, anti-biofilm activity of zinc oxide nanoparticles on bacteria isolated from burns infection*, AIP Conf. Proc. 3190 (2025) 030005.
14. Q. Al-Obaidi, M.S. Mahmoud, R. Nabil, *Study of prototypes for biofuel production Extraction from biodegradation in oxygen-free environments Processing Wastewater*, Sol. Energy Sustain. Dev. J. 14 (2025) 522–539.
15. S. Doyurum, *A. Çelik, Pb (II) and Cd (II) removal from aqueous solutions by olive cake*, J. Hazard. Mater. 138 (2006) 22–28.
16. T.A. Abdullah, Q. Al-Obaidi, T.A. Abdulla, R.T. Rasheed, K. Al-Azawi, F. Meharban, *A Critical Review of the Photocatalytic Degradation of Pharmaceutical Residues by a TiO_2-Based Photocatalyst*, Hung. J. Ind.

Chem. 51 (2023) 65–75.

17. T.A. Abdullah, H.L. Khaleel, A.W. Saeed, M.N. Mohammed, Q. Al-Obaidi, M.A. Hussein, W.A. Mhmood, R.T. Rasheed, O.I. Abdullah, *Experimental Analysis of rGO-V_2O_5 Nanocomposites for Sustainable Water Remediation Completed with Bibliometric Analysis Toward Achieving Sustainable Development Goals (SDGs)*, ASEAN J. Sci. Eng. Mater. 5 (2026) 267–286.
18. Q. Al-Obaidi, M. Alabdulmuhsin, A. Tolstik, J.G. Trautman, M. Al-Dahhan, *Removal of hydrocarbons of 4-Nitrophenol by emulsion liquid membrane (ELM) using magnetic Fe2O3 nanoparticles and ionic liquid*, J. Water Process Eng. 39 (2021) 101729.
19. M. Sekar, V. Sakthi, S. Rengaraj, *Kinetics and equilibrium adsorption study of lead(II) onto activated carbon prepared from coconut shell*, J. Colloid Intersface Sci. 279 (2004) 307–313.
20. A.M. Rdhewa, I. Karim, Z.B. Mohammed, *Changes in groundwater levels and its salinity (Badra Basin Iraq)*, IOP Conf. Ser.: Earth Environ. Sci. 1232 (2023) 012061.
21. A.M. El-Wakil, W.M. Abou El-Maaty, F.S. Awad, *Removal of Lead from Aqueous Solution on Activated Carbon and Modified Activated Carbon Prepared from Dried Water Hyacinth Plant*, J. Anal. Bioanal. Tech. 5 (2014) 1000216.
22. F.A. Abdulkareem, G.H. Mohamed, A.S. Resheq, Z. Bahaa, *Assessment the performance of water treatment plants in Baghdad governorate using GIS, Period*. Eng. Nat. Sci. 10 (2022) 228–238.
23. Ni'Mah, Lailan, Sri Rachmania Juliastuti, and Mahfud Mahfud. *"One-stage microwave-assisted activated carbon preparation from Langsat peel raw material for adsorption of iron, manganese, and copper from acid mining waste."* Commun. Sci. Technol. 8 (2023) 143-153.
24. H. Talib Hamzah, V. Sridevi, M. Seereddi, D.V. Suriapparao, P. Ramesh, C. Sankar Rao, R. Gautam, F. Kaka, K. Pritam, *The role of solvent soaking and pretreatment temperature in microwave-assisted pyrolysis of waste tea powder: Analysis of products, synergy, pyrolysis index, and reaction mechanism*, Bioresour. Technol. 363 (2022) 127913.
25. Thamer Adnan Abdullah, Qusay Al-Obaidi, Thaer A. Abdulla, Rashed T. Rasheed, Khalda Al-Azawi, and Faiza Meharban. *A Critical Review of the Photocatalytic Degradation of Pharmaceutical Residues by a TiO_2-Based Photocatalyst*. Journal of Hungarian Journal of Industry and Chemistry. 51 (2023) 65–75.
26. Y.a.J.A. Hamadani, A.M. Salal, Z. Bahaa, L.N. Assi, A.S. Resheq, *WQ assessment of water treatment plants using environmental and statistical indicators within Baghdad City*, Period. Eng. Nat. Sci. 10 (2022) 427–438.
27. M.A. Ali, S.A. Mahdy, N.N. Hussein, *Anticancer Properties of Titanium Dioxide (TiO2) Nanoparticles Obtained from Quercus infectoria Plant Extract*, J. Nanostructures 14 (2024) 492–504.
28. M.A. Ali, S.A. Mahdy, N.N. Hussein, *Synthesis of Titanium Dioxide Nanoparticles (TiO2) and Application for Reduction of Bacterial Growth*, J. Nanostructures 14 (2024) 1046–1057.
29. P. Barpanda, G. Fanchini, G.G. Amatucci, *Structure, surface morphology and electrochemical properties of brominated activated carbon*s, Carbon 49 (2011) 2538–2548.
30. F.M. Abdulla, Z.Y. Shnain, A.A. Alwasiti, M.F. Abid, N.H. Abdurahman, *Photocatalysis technology for treating petroleum wastewater and the potential application of tapered bubble column (TBC): a review*, Global NEST J. 26 (2024) 05681.
31. F.A. Abdulkareem, G.H. Mohamed, A.S. Resheq, Z. Bahaa, *Assessment the performance of water treatment plants in Baghdad governorate using GIS*, Period. Eng. Nat. Sci. 10 (2021) 228.
32. M.N. Mohammed, O.I. Abdullah, M.J. Jweeg, H.S.S. Aljibori, T.A. Abdullah, N.M. Alawi, R.T. Rasheed, F. Meharban, H.T. Hamzah, Q. Al-Obaidi, *Comprehensive Review on Wastewater Treatment Using Nanoparticles: Synthesis of Iron Oxide Magnetic Nanoparticles, Publication Trends via Bibliometric Analysis, Applications, Enhanced Support Strategies, and Future Perspectives*, ASEAN J. Sci. Eng. 5 (2025) 1–30.
33. Y. Wang, T. Zhang, X. Wang, *Removal mechanism of lead by the composite of clinoptilolite, biochar, and Ca(OH)2 and its application in acid wastewater,* Environ. Technol. Innov. 37 (2025) 104024.
34. F.C. Wu, R.L. Tseng, R.S. Juang, *Characteristics of functional groups of adsorbents and their effects on the adsorption mechanism*, J. Hazard. Mater. 364 (2019) 482–491.
35. T.A. Saleh, *Adsorption isotherms and kinetic models: fundamentals and recent developments*, Environ. Nanotechnol. Monit. Manag. 20 (2023) 10012.
36. Z. Zhang, et al., *Adsorption of heavy metal ions on activated carbon prepared from agricultural wastes*, Bioresour. Technol. 313 (2020) 123634.
37. G. Enaime, A. Baçaoui, A. Yaacoubi, *Adsorption properties of activated carbon prepared from biomass waste*, J. Environ. Chem. Eng. 8 (2020) 103146.
38. A.M. El-Wakil, W.M. Abou El-Maaty, F.S. Awad, *Removal of lead from aqueous solution on activated carbon and modified activated carbon prepared from dried water hyacinth plant*, J. Anal. Bioanal. Tech. 5 (2014) 1000187.
39. K. Li, Z. Zheng, Y. Li, *Characterization and lead adsorption properties of activated carbons prepared from cotton stalk by one-step H3PO4 activation*, J. Hazard. Mater. 181 (2010) 440–447.
40. M.A. Akl, A.G. Mostafa, M. Al-Awadhi, W.S. Al-Harwi, A.S. El-Zeny, *Zinc Chloride Activated Carbon Derived from Date Pits for Efficient Biosorption of Brilliant Green: Adsorption Characteristics and Mechanism Study*, Appl. Water Sci. 13 (2023) 226.
41. B. Wang, J. Lan, C. Bo, B. Gong, J. Ou, *Adsorption of heavy metal onto biomass-derived activated carbon*, RSC Adv. 13 (2023) 4275–4302.
42. M. Ulfa, R.F. Hanif, N.A. Sholeha, *Surface chemistry and adsorption behavior of methylene blue on functionalized carbon materials: a comprehensive study*, Commun. Sci. Technol. 10 (2025) 276–291.
43. J. Humadi, A.T. Nawaf, L.A. Khamees, Y.A. Abd-Alhussain, H.F. Muhsin, M.A. Ahmed, M.M. Ahmed, *Development of new effective activated carbon supported alkaline adsorbent used for removal phenolic compounds*, Commun. Sci. Technol. 8 (2023) 164–170.